EASR

Engineering and Applied Science Research

https://www.tci-thaijo.org/index.php/easr/index

Published by the Faculty of Engineering, Khon Kaen University, Thailand

Study of air distribution in tray dryer using computational fluid dynamics

Manop Rakyat[1)], Pracha Yeunyongkul[2)], Korawat Wuttikid[2)], Surapin Promdan[2)], Nawee Nuntapap[2)], Chatchawan Chaichana[3)], Arpiruk Hokpunna[3)], Thatchapol Chungcharoen[4)], Nuttapong Ruttanadech[4)], Prathan Srichai[5)] and Ronnachart Munsin*[1, 2)]

[1)]Sustainable Technology Research Laboratory, Department of Mechanical Engineering, Faculty of Engineering, Rajamangala University of Technology Lanna, Chiang Mai 50300, Thailand
[2)]Applied Thermal-Fluid Research Group, Department of Mechanical Engineering, Faculty of Engineering, Rajamangala University of Technology Lanna, Chiang Mai 50300, Thailand
[3)]Department of Mechanical Engineering, Faculty of Engineering, Chiang Mai University, Chiang Mai 50200, Thailand
[4)]Department of Engineering, King of Mongkut's Institute of Technology Ladkrabang, Prince of Chumphon Campus, Chumphon 86160, Thailand
[5)]Department of Mechanical Engineering, Faculty of Engineering, Princess of Naradhiwas University, Narathiwat 96000, Thailand

Received 19 March 2021
Revised 11 April 2021
Accepted 13 May 2021

Abstract

The objective of this work is to investigate the air flow distribution in conventional tray dryer and modified dryer using computational fluid dynamics. Simplified model of drying chamber with assumptions was used for simulation. Grid independence study and model validation were performed with the model of conventional tray dryer. Relative error of models was acceptable for all simulations. The shape of front and rear walls of drying chamber was varied. The results showed that the reason of poor air distribution inside conventional tray dryer was improper installation of air baffle resulting in air flow obstruction. Flow pattern inside the modified drying chamber highly depends on the front wall, while effect of rear wall on flow was insignificant. The critical zones occur at the top of drying chamber for both conventional and modified tray dryers.

Keywords: Tray dryer, Computational fluid dynamics, Grid independence study, Validation

1. Introduction

Agricultural products are important goods in the global markets. A supply of agricultural product is abundant during the harvest. To preserve and add value of products, hot air drying is most favorite. The multi-purpose tray dryer or fixed-bed dryer is widely used with ranges of operating and reasonable cost, especially in small business. However, heterogeneity of air flow inside dryer is usually observed in the dryer resulted poor products [1, 2]. Switching of tray during drying process is required to improve air distribution in the practical use. It is clear that the air flow distribution inside dryers plays an important role in quality of product. Several works experimentally introduced new techniques for improving air distribution, e.g. hot air recirculation [3-5], diagonal-airflow batch dryer [6], the combination of various heat sources, including heat pump, solar and infrared, for a drying system [7], the dryer mixed with solar [8] and dryer combined with geothermal system [9]. Unfortunately, the experimental studies for improving air flow distribution in dryers are tough, costly and time consuming [10, 11].

To reduce the limitation of flow study by experiment, computational fluid dynamics (CFD) is used as a tool for predicting flow behavior with low cost and short time [12-14]. CFD was introduced in the drying areas with varieties of study. Results from CFD analyzing showed that shape parameters caused uneven air distribution in dryer [1, 2, 15-17]. Different complex geometry of full-scale industrial dryer affected on quality of dried product and energy consumption. The optimal parameter of dryer shapes increased 23% in the uniformity of final product moisture [18]. The improvement of air distribution in a tray dryer can be done by new design with the expanded inlet, resulting 50% reduction of span of moisture content compared to the convention tray dryer [2]. The air baffles or air guides at entrance also showed good drying uniformity [11]. Air flow rate controls not only drying time but also uneven drying [19, 20]. From the literature, it can be summarized that the dryer geometry are important parameters. The distribution of air flow depending on design has influence on drying quality. New design of drying chamber, especially entrance and exit walls, is necessary. The optimum parameters vary from case to case shown in the literature. It is difficult to apply the same optimum parameters to the others which have the different sizes, shapes, products and functions of operating. This is a limitation of tray dryer in practice. In addition, there have not been previous works that investigate the effect of the entrance and rear walls with the simple stack of tray in the regular compact tray dryer on air flow distribution. Therefore, the objective of this work is to investigate effect of wall shapes on the air flow distribution of the modified dryer. Flow characteristics can be used to improve the overall performance of the tray dryer leading to decreasing of time and operating cost.

*Corresponding author. Tel.: +66 5392 1444
Email address: ronnachart@rmutl.ac.th
doi: 10.14456/easr.2021.69

2. Materials and methods

2.1 Conventional tray dryer and 3D model

Figure 1 (a) and (b) show the multi-purpose conventional tray dryer and its diagram, respectively, consisting of inlet, outlet, burner, controller, blower, drying chamber and stacks of tray. Air flow rate and temperature were automatically controlled by a controller. Drying capacity of dryer is in the range of 90-100 kg depending on agricultural products, e.g. longan, mango, banana and lychee. During drying process, air moves into tray dryer at the top. Then, air is heated at the plenum by burner before it moves into drying chamber where it contains separately 18 trays shown in Figure 2. Heated air passes through stacks of tray, and it shifts upward moving out of dryer at the exit on the top. To reduce complexity of CFD model and computational time, only drying chamber (dimensions 114.5×239.0×90.0 cm) will be considered as CFD model shown in Figure 3 (a). Afterwards, model discretization is performed to generate mesh in Figure 3 (b).

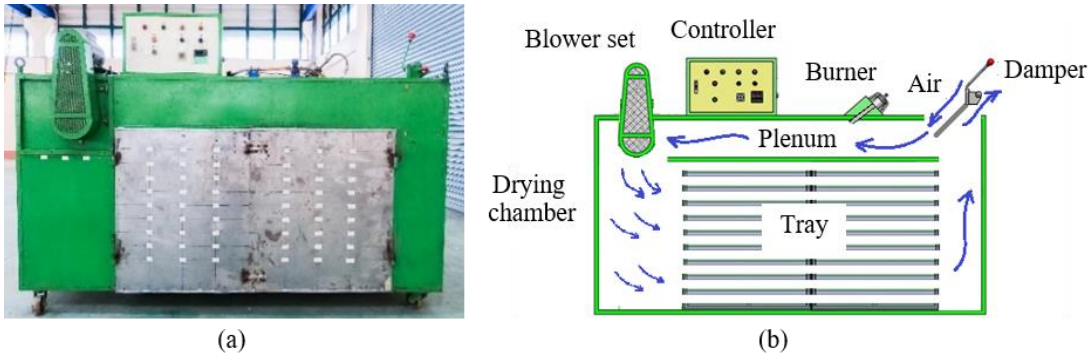

Figure 1 (a) Conventional tray dryer and (b) Diagram of conventional tray dryer

Figure 2 Trays inside the tray dryer

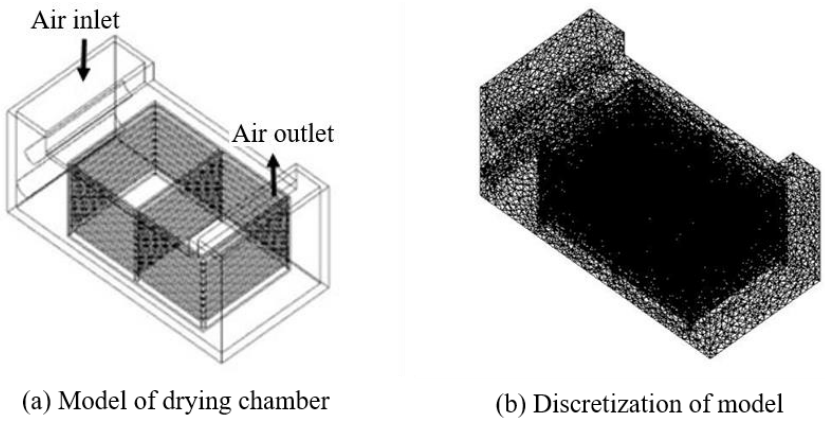

Figure 3 Tray dryer model for CFD simulation

2.2 Computational fluid dynamics

Flow simulations in this work were performed by the CFDRC V2004. The governing equations for simulation are shown in equation (1)-(3) [21]. The standard k-ε model was employed for turbulent flow calculation based on transport equation for the turbulence kinetic energy (k) and its dissipation rate (ε) shown in [22]. In simulation, the assumptions to reduce the complexity of calculation are made following:

- Air flow in the dryer is steady state-steady flow condition.
- Inlet air has a uniform velocity.
- Incompressible flow and constant air density are reasonably used for the models, because maximum air velocity in the dryer is much far from sound speed in the air. This means that Mach number of air flow in dryer is much smaller than 0.1 [2]. Viscosity of air in dryer is also kept constant for the models.
- No-slip wall condition is considered at the wall surface.
- When the product is fully loaded to the trays, very small amount of air can vertically pass through the trays. Therefore, air flow in the parallel direction to the trays is only considered. In the simulation model, the trays are considered as impenetrable trays.

Continuity equation: $\frac{\partial \rho}{\partial t} + \nabla \cdot (\rho \vec{v}) = 0$ (1)

Momentum equation $\frac{\partial}{\partial t}(\rho \vec{v}) + \nabla \cdot (\rho \vec{v} \vec{v}) = -\nabla p + \nabla \cdot (\vec{\tau}) + \rho \vec{g} + \vec{F}$ (2)

Energy equation $\frac{\partial}{\partial t}(\rho E) + \nabla \cdot \left(\vec{v}(\rho E + p)\right) = \nabla \cdot \left(k_{eff} \nabla T\right) + S_h$ (3)

Where $\rho, t, \vec{v}, p, \vec{\tau}, g, \vec{F}, E, k_{eff}, T$ and S_h are, respectively, density (kg/m^3), time (*sec*), flow velocity (*m/sec*), pressure (Pa), stress tensor (Pa), gravity (m/sec^2), momentum sink term (Pa), total energy (J), effective conductivity (J/mK), temperature (K) and volumetric heat source (Pa/sec).

2.3 Conditions for simulation

To study the flow inside the air dryer by CFD, some processes are required before the model simulation. Grid independence study is initially performed. Then model validation are carried out. Finally, air flow distribution of modified tray dryer is investigated.

2.3.1 Grid independence study

Grid independence have to be studied initially for the simulation model of the conventional tray dryer. The optimum grid cells in the model not only play an important role on reliable results but also affect computational time [23]. Different grid cells were refined from 42,504 to 707,486 cells. The result for each number of cells was averaged from all data on the center plane of model. Grid independence will be obtained when insignificant change in the results is noticed with the increase of number of grid cells. The optimum grid cells will be used throughout the simulations including validation and modified tray dryer.

2.3.2 Model validation

Model validation can be performed by comparison of extracted data between experiments and simulations at the same operating conditions of the conventional tray dryer. In experiment, air velocities were measured by hot wire anemometer Jedto model AFM029 with accuracy ±3%. The measurement positions of air velocity is shown in Figure 4. Measurement for each point was repeated 5 times to find the average velocity.

The experimental data at inlet and outlet of dryer was used for the boundary conditions of the model shown in Table 1. At inlet, air velocity in y-direction and temperature were kept constant at 6.17 m/s and 343 K, respectively. Air exits the outlet where atmospheric pressure and ambient temperature were assigned. Turbulence kinetic energy and dissipation rate of inlet and outlet were 0.01713 m^2/s^2 and 0.002631 m^2/s^3, respectively. The convergence of numerical solutions will be obtained by 2 criteria, i.e. the number of iterations of 5,000 cycles and the residual values of 0.0001 for all variables.

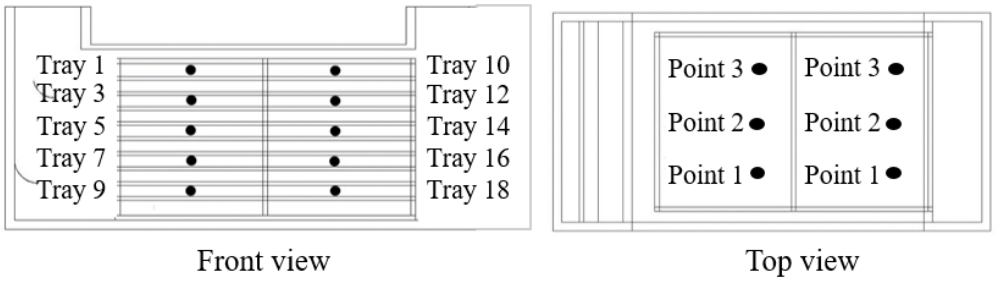

Figure 4 Positions for measuring velocity inside the drying chamber

Table 1 Boundary conditions for model validation

Inlet	Outlet
Cartesian (X,Y,Z)	Fixed Pressure
U = 0 m/s, V = 6.17 m/s ,W = 0 m/s	Gauge Pressure = 0
T= 343K	T =300K
Standard k-ε	Standard k-ε
Turbulence kinetic energy 0.01713 m^2/s^2	Turbulence kinetic energy 0.01713 m^2/s^2
Turbulence dissipation rate 0.002631 m^2/s^3	Turbulence dissipation rate 0.002631 m^2/s^3

2.3.3 Flow investigation of modified tray dryer

Initially, flow pattern of the conventional air dryer model showing in Figure 3 was investigated to explain flow behaviors causing poor drying. Then new design of front (entrance) and rear walls was introduced as shown in Figure 5, while tray positions were fixed for all simulations. The radius of front and rear walls were varied. The air baffles at entrance using in the conventional tray dryer were removed in the modified tray dryer. Details of modification are shown in Table 2. Boundary conditions of the modified dryer were exactly same as the validation case. Flow characteristics deriving from the simulations will be used as parameters for assessing the improvement of air distributions.

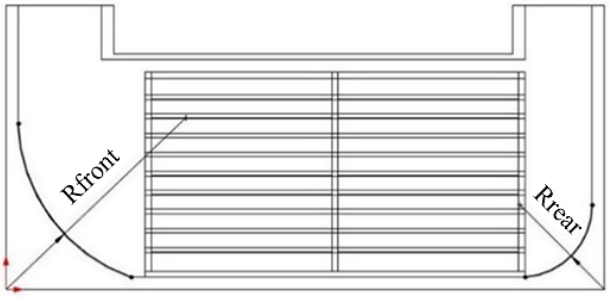

Figure 5 New design of tray dryer

Table 2 Geometrical parameters of modified tray dryer

Parameters	Case					
	A	**B**	**C**	**D**	**E**	**F**
Radius of front walls (cm)	48	70	104	-	-	70
Radius of rear walls (cm)	-	-	-	30	50	30

Heterogeneity of air flow distribution inside tray dryer can be represented by the velocity span as shown in Figure 6. To assess the overall performance of the modified tray dryer, the velocity span will be used. Smaller velocity span allows the better air flow distribution resulting in the uniformity of drying rate and quality of products [18]. It is noticed that tray 1 and 10 were excluded from the velocity span, because they are critical zones, where they show very low velocity for tray 1 and high variation of velocity for tray 10 in all cases.

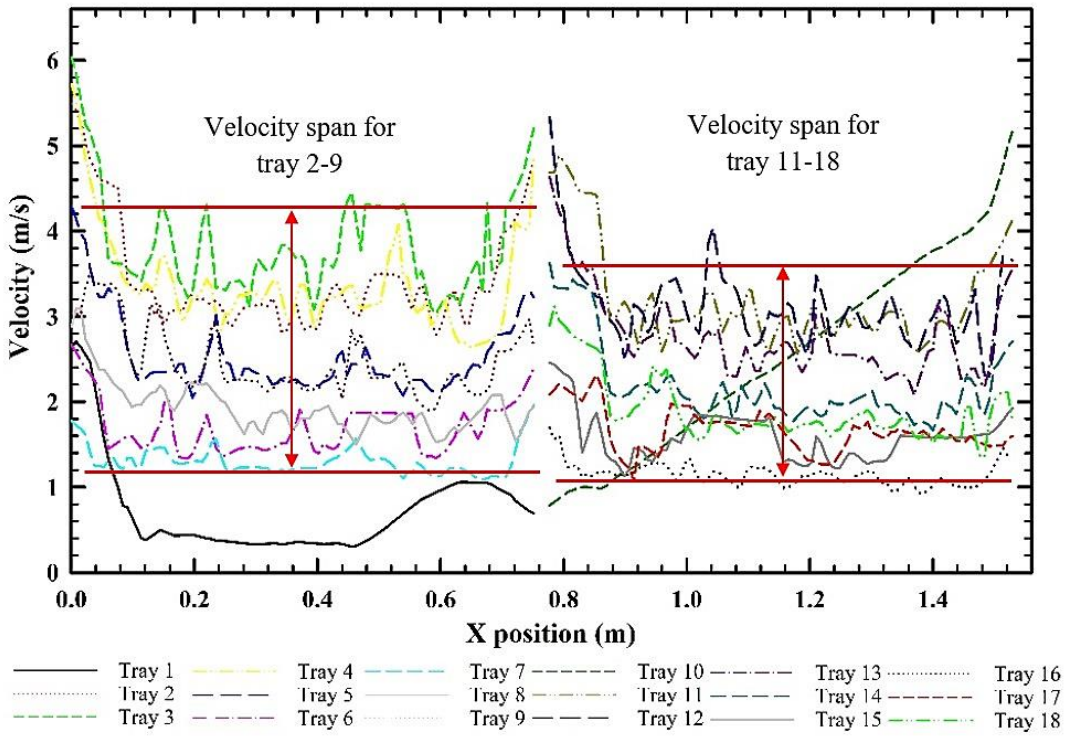

Figure 6 Velocity span

3. Results and discussions

3.1 Grid independence study and model validation

Effect of grid cells on the velocity magnitude is shown in Figure 7 (a). The increase in number of cells directly impacts on velocity magnitude in the region 1, but it shows insignificant variation of velocity magnitude in the region 2. Grid independence was met in this region beyond the grid cell of 474,063. Therefore, the present study uses this number of cell to perform throughout simulations.

Model validation was investigated by the comparison of extracted data of the experiment and simulation shown in Figure 7 (b). Simulation results showed a strong correlation and reasonably match to those of the experiments. Averaged relative error is about of 16.64%. The errors are probably from assumptions made and the local complexity of tray dryer. The accuracy criteria in [24] suggests that if the relative error is less than 20-30% the simulation results are rated as B and acceptable. Therefore, it can be implied that the CFD model with 16.64% relative error is suitable to predict flow in the conventional tray dryer.

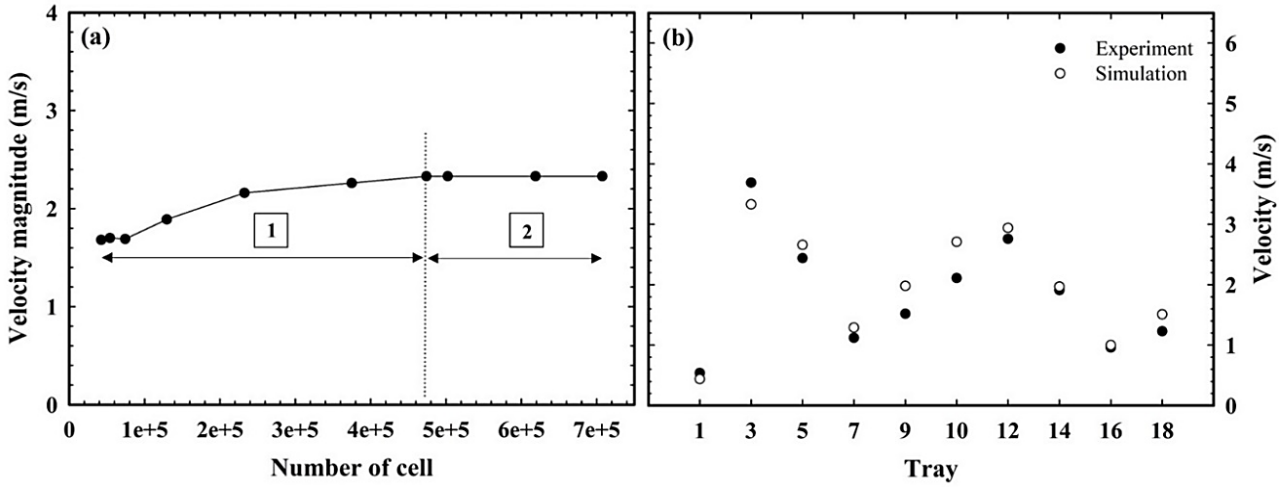

Figure 7 (a) Effect of grid cells on the velocity magnitude and (b) Model validation

3.2 Flow investigation of conventional tray dryer

Figure 8 (a) – (d) show the simulation results of the conventional tray dryer. In Figure 8 (a), the simulation reveals that there is a large difference in velocity between upper and lower trays. The critical or dead zone is above the highest trays, i.e. tray 1 and 10, where the lowest velocity is in the range of 0.4-1 m/s, on the other hand, the range of highest velocity (3.5-6 m/s) is noticed at the tray 2-5 and 11-13 as shown in Figure 8 (c). The similar observation was reported in other works [11, 13] that studied flow inside tray dryer. Vorticity, representing the local spinning motion, is a parameter for flow analysis. Low vorticities above tray 1 and 10 showing in Figure 8 (b) and (d) also confirm that critical zone occurs in these regions. Beside of tray 1 and 10, other critical zones are observed at the middle of tray stacks, i.e. tray 6, 7, 15 and 16. So, the critical zone could be defined as where it has low velocity and vorticity. The explanation for critical zone occurrences is postulated that the downward inlet air, containing high inertia force, cannot immediately change direction to the tray 1 and 10 although air baffles was installed at the entrance. Surprisingly, air baffles at the entrance block the flow for the others, resulting in the lower critical zones. With this flow behavior, the products located at the critical zone would receive insufficient energy and could not be dried, while the others receiving overflow are exceedingly dried, because drying air temperature and velocity play an important role on the dehydration rate [25, 26]. These results could be used to explain why heterogeneous products were obtained when this tray dryer was used for drying of agricultural products.

3.3 Flow simulation of modified tray dryer

Modification of the drying chamber shape shows significant effect on air velocity distribution illustrated in Figure 9 to Figure 12. In case A to C, the air baffles occurred in the conventional tray dryer were removed, and the front radius of entrance wall was varied, while rear walls are same to the conventional dryer. In comparison with the conventional tray dryer, it was found that front radius of entrance wall without air baffle shows the promising results. Air distribution, showing in Figure 9 and Figure 10, seems more homogenous throughout the trays except tray 1 and 10, where the critical zones still remain as well as the conventional tray dryer. There is insignificant difference in air flow results among case A to C. This is confirmed by the comparison of improvement, determining from air velocity profile in Figure 9 and difference of velocity in Figure 10, for each individual tray between the conventional and modified tray dryer shown in Table 3. However, if considering vorticity in Figure 11 and Figure 12, case B seems slightly better than the others particularly tray 1 and 10. it could be implied that more turbulence, increasing in drying rate, occurred in case B. Case D and E shows effect of rear wall with two different radius on flow characteristics, while front walls are exactly same to the conventional dryer. Air velocities in case D and E over trays were almost same to that of conventional dryer. On the contrary, air velocity profile and vorticity over tray 1 were terrible in case E. Case F is the modification of front and rear wall radius. The results show the improvement of both flow and vorticity inside drying chamber as case A and B. However, the critical zones on tray 1 and 10 still occurred.

From the simulation results, Case B seems to be better than the others considering from such as the structure, uniformity in air flow distribution and vorticity. However, the dead zones still remain at the top of drying chamber. A suggestion for the future work is about other design to improve flow at the critical zone. In addition, the porous model will be applied for trays.

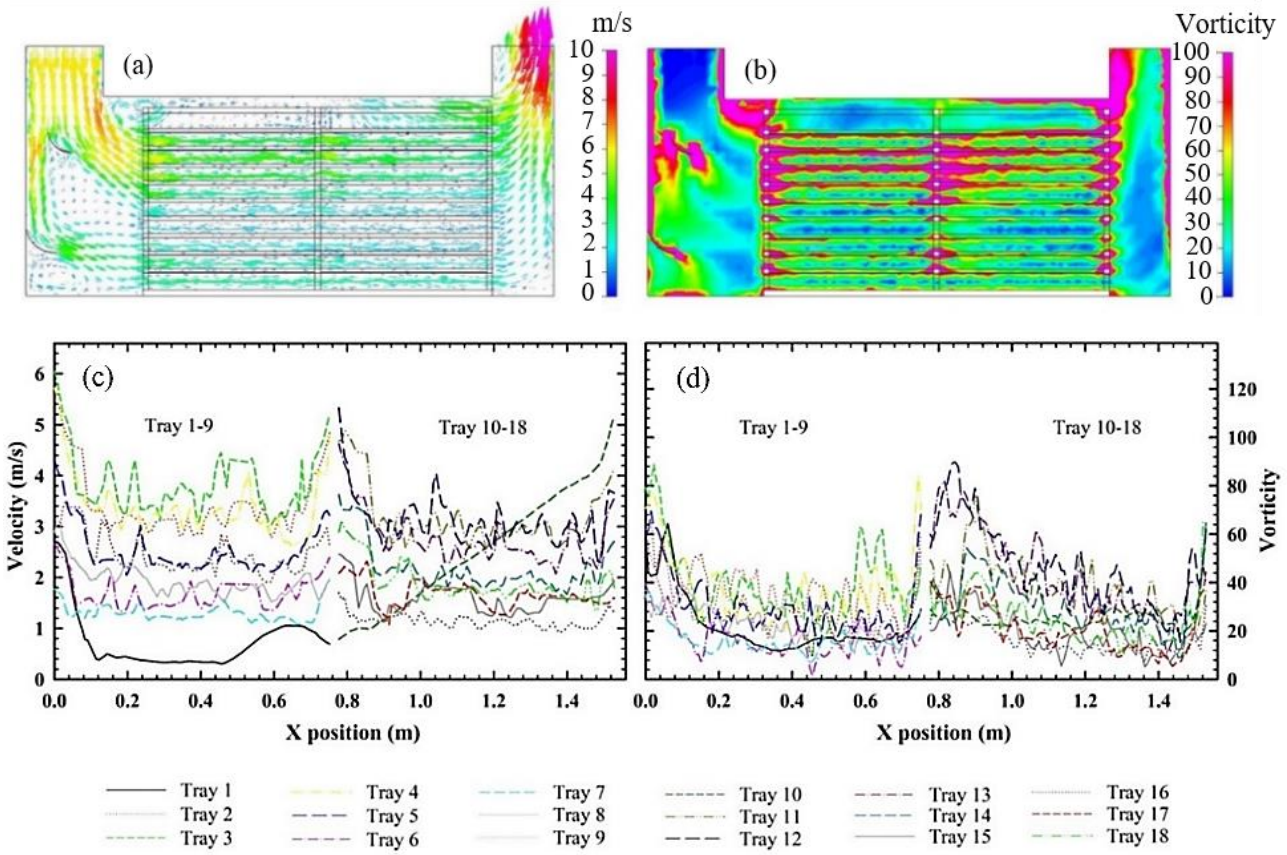

Figure 8 Simulation results of the conventional tray dryer; (a) air flow pattern, (b) contour of vorticity, (c) air velocity at 3.0 cm above trays along x-position (length of chamber) and (d) vorticity at 3.0 cm above trays along x-position

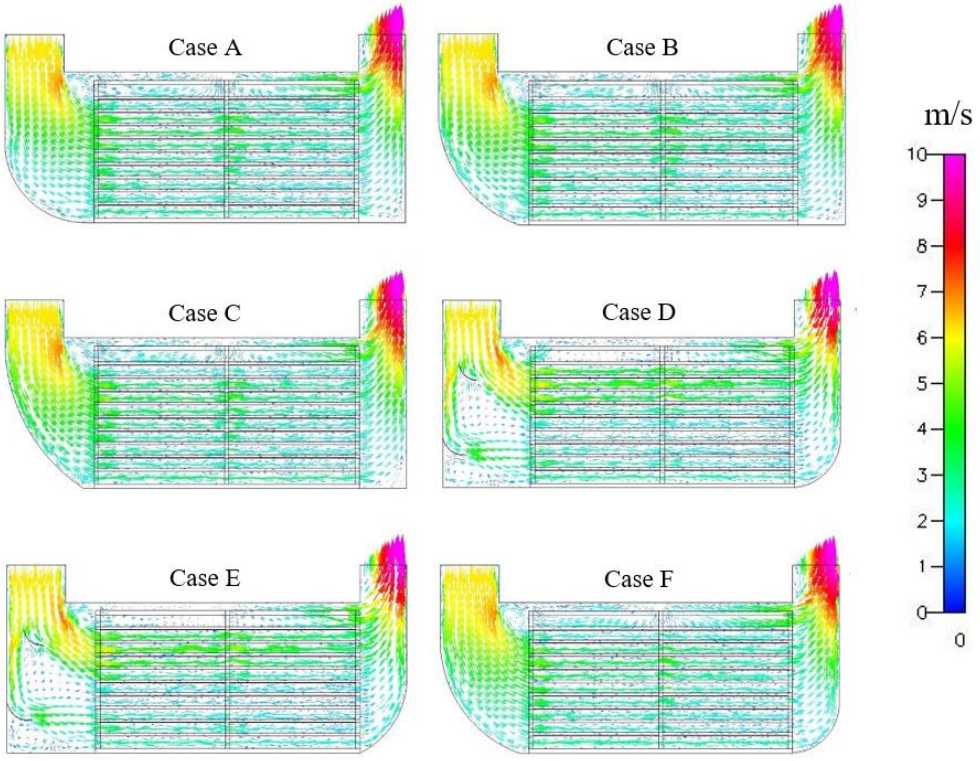

Figure 9 Air flow pattern inside modified tray dryers

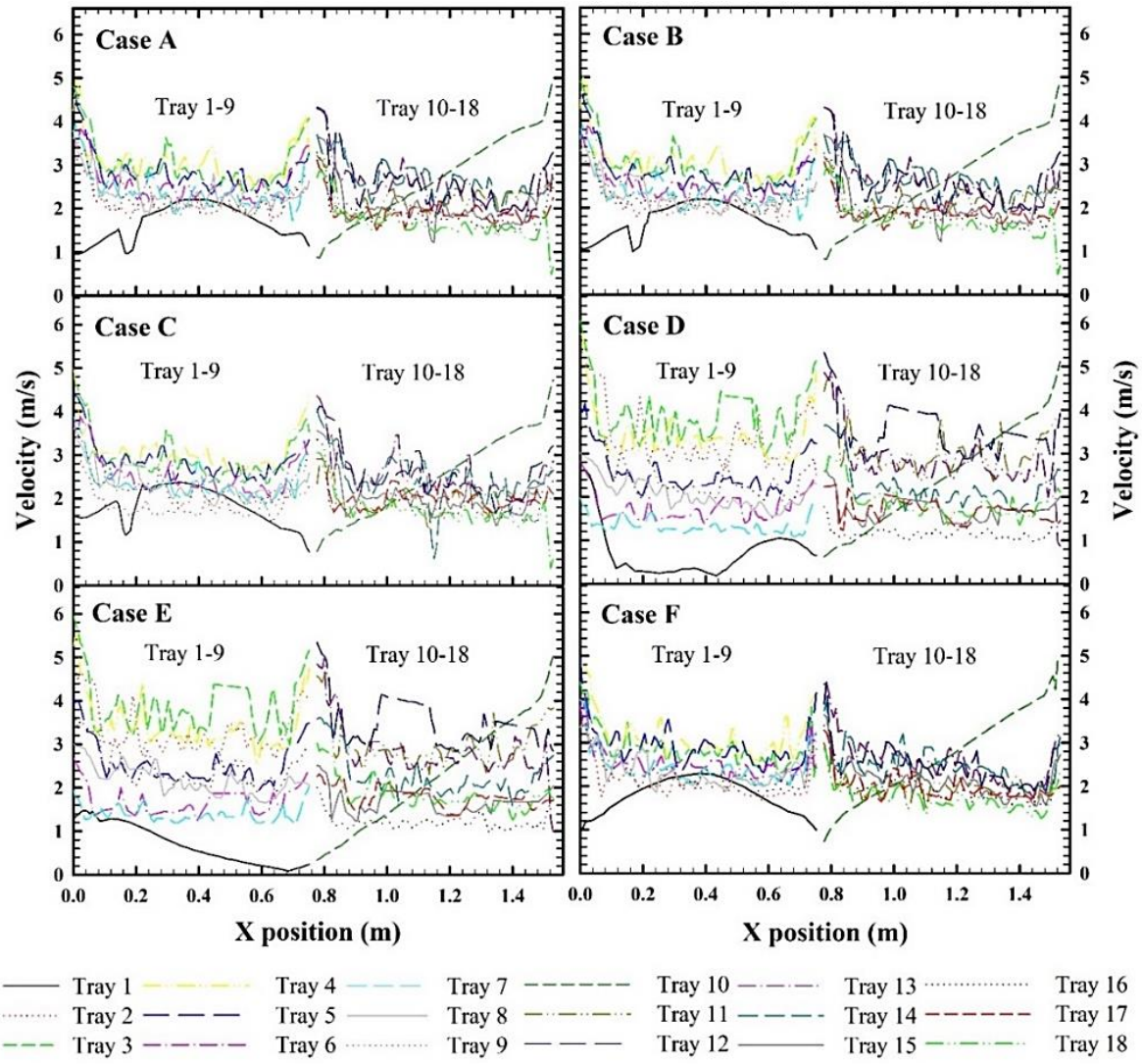

Figure 10 Air velocity at 3.0 cm above trays along x-position for modified tray dryers

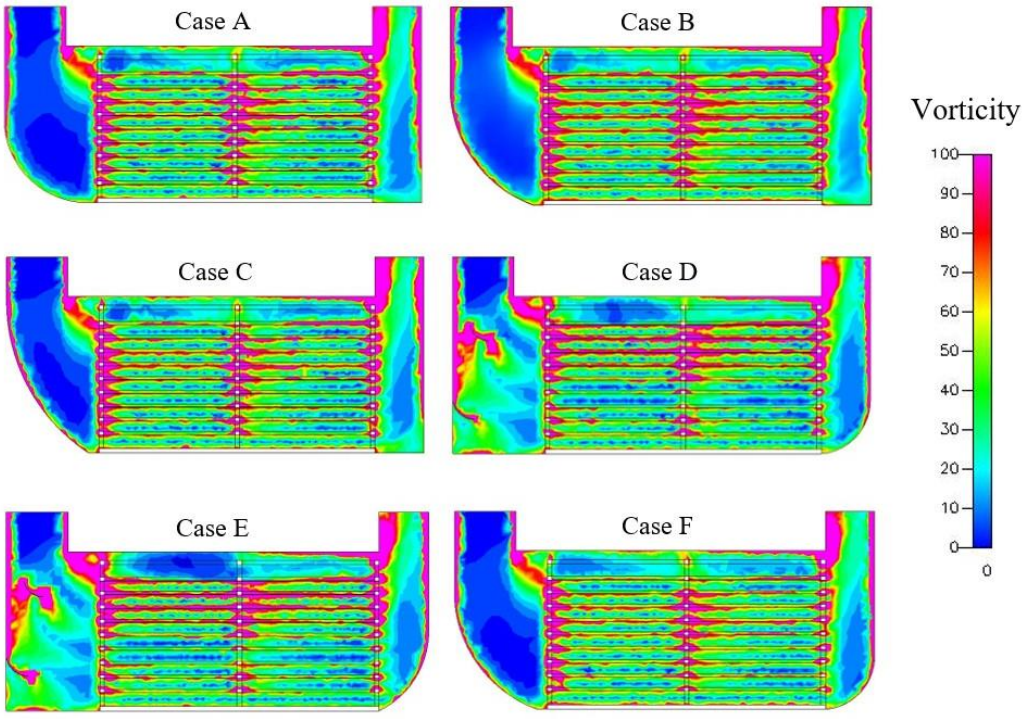

Figure 11 Contour of vorticity inside modified tray dryers

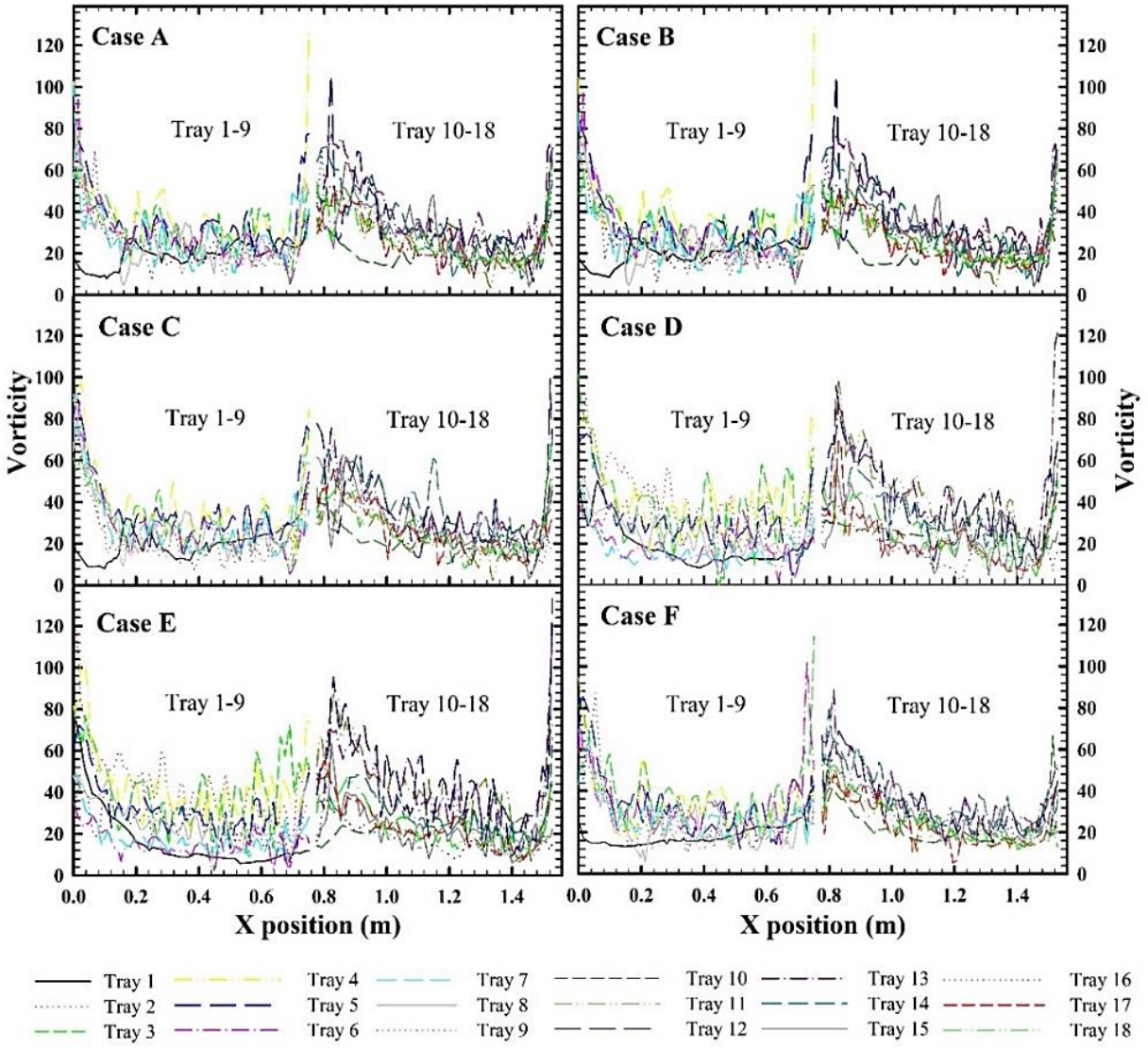

Figure 12 Vorticity at 3.0 cm above trays along x-position for modified tray dryers

Table 3 Comparison of the improvement of velocity profile between the conventional and modified tray dryer

Case	Front (cm)	Rear (cm)	Tray																	
			1	2	3	4	5	6	7	8	9	10	11	12	13	14	15	16	17	18
A	R=48	Conventional wall	0	+	+	+	+	+	+	+	+	0	+	+	+	+	+	+	+	+
B	R=70	Conventional wall	0	+	+	+	+	+	+	+	+	0	+	+	+	+	+	+	+	+
C	R=104	Conventional wall	0	+	+	+	+	+	+	+	+	0	+	+	+	+	+	+	+	+
D	Conventional wall	R=30	0	0	+	0	0	0	0	0	0	0	0	-	0	0	0	0	0	0
E	Conventional wall	R=50	-	0	+	0	0	0	0	0	0	0	0	-	0	0	0	0	0	0
F	R=70	R=30	0	+	+	+	+	+	+	+	+	0	+	+	+	+	+	+	+	+

Note: (-) is worse than the conventional dryer. (0) is no change. (+) is better than the conventional dryer.

Figure 13 shows velocity span of the tray dryers extracted from air velocity profile. In comparison of the velocity span of the conventional and modified tray dryers, it was found that the tray dryers with modification of entrance wall in case A and B show the highest reduction of velocity span by 45% and 32% for tray 2-9 and 11-18, respectively, while there is no improvement in case of modification of rear walls (case D and E) for tray 2-9. In addition, case D and E expands the velocity span for tray 11-18 by 24%. These results can be postulated that the overall performance of the modified tray dryer will be improved in case of lower velocity span compared with the conventional tray dryer, because the decrease of velocity span allow the better air flow distribution. In other words, the similar drying rate for each tray can be obtained by small velocity span resulting in homogeneity of products [2, 11, 18, 19] and decrease of drying time [19].

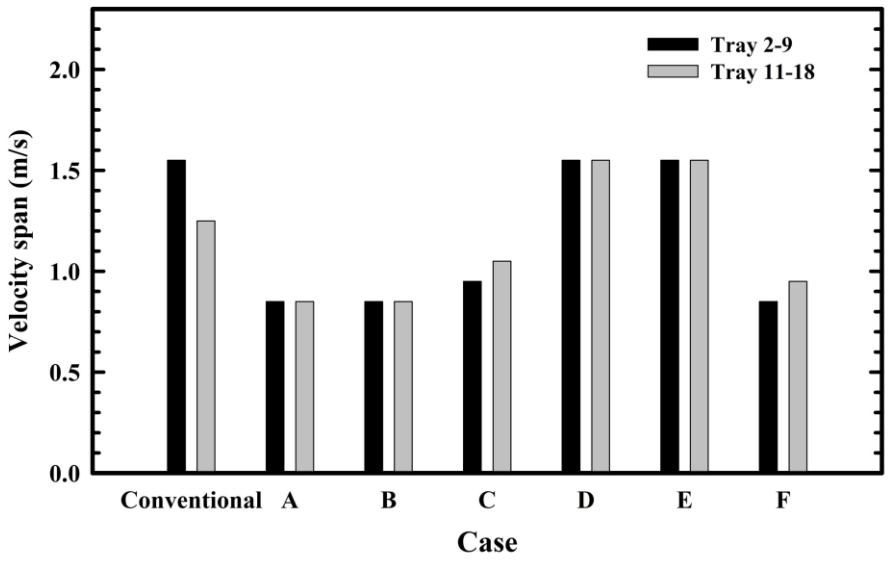

Figure 13 Velocity span of the tray dryers

4. Conclusions

In this study, simulations using computational fluid dynamics were performed to investigate the flow characteristics of tray dryer. The optimum grid cells were obtained by grid independence study before model validation and simulation of other design of drying chamber. The average relative error of CFD models is about of 16.64% which is acceptable for simulation. The results showed that in case of the conventional tray dryer, poor air distribution comes from the obstruction of air baffle located at the entrance. The critical zones are at the top of drying chamber and the middle of stack of trays, where air flow was blocked by the air baffle. For the modified tray dryer, it is clear that front wall drastically improves flow characteristics inside drying chamber, while rear wall has slightly effects on flow. A more uniform air distribution occurred in case B (radius of front wall of 70 cm). However, the critical zones still remain at the top of drying chamber.

5. Acknowledgements

The authors highly acknowledge Rajamangala University of Technology Lanna and Chiang Mai University for supporting facilities and CFD software. A technical staff of Chiang Mai Agricultural Engineering Research Center is also gratefully acknowledged for their help during the experimental works.

6. References

[1] Amanlou Y, Zomorodian A. Applying CFD for designing a new fruit cabinet dryer. J Food Eng. 2010;101(1):8-15.
[2] Román F, Strahl-Schafer V, Hensel O. Improvement of air distribution in a fixed-bed dryer using computational fluid dynamics. Biosystems Eng. 2012;112(4):359-69.
[3] Tippayawong N, Tantakitti C, Thavornun S, Peerawanitkul V. Energy conservation in drying of peeled longan by forced convection and hot air recirculation. Biosystems Eng. 2009;104(2):199-204.
[4] Das S, Das T, Rao PS, Jain RK. Development of an air recirculating tray dryer for high moisture biological materials. Food Eng. 2001;50(4):223-7.
[5] Mohammadi I, Tabatabaekoloor R, Motevali A. Effect of air recirculation and heat pump on mass transfer and energy parameters in drying of kiwifruit slices. Energ. 2019;170:149-58.
[6] Amjad W. Design and development of a diagonal- airflow batch dryer for spatial drying homogeneity [dissertation]. Witzenhausen: University of Kassel; 2016.
[7] Singh A, Sarkar J, Sahoo RR. Experimental performance analysis of novel indirect-expansion solar-infrared assisted heat pump dryer for agricultural products. Sol Energ. 2020;206:907-17.
[8] Djebli A, Hanini S, Badaoui O, Boumahdi M. A new approach to the thermodynamics study of drying tomatoes in mixed solar dryer. Sol Energ. 2019;193:164-74.
[9] Chaiyat N. A multigeneration system of combined cooling, heating, and power (CCHP) for low-temperature geothermal system by using air cooling. Therm Sci Eng Progr. 2021;21:1-12.
[10] Mirade PS. Prediction of the air velocity field in modern meat dryers using unsteady computational fluid dynamics (CFD) models. Food Eng. 2003;60:41-8.
[11] Misha S, Mat S, Ruslan MH, Sopian K, Salleh E. The CFD simulation of tray dryer design for Kenaf core drying. Appl Mech Mater. 2013;393:717-22.
[12] Norton T, Sun DW. Computational fluid dynamics (CFD) an effective and efficient design and analysis tool for the food industry: a review. Trends Food Sci Tech. 2006;17(11):600-20.
[13] Anand S, Mishra DP, Sarangi SK. CFD supported performance analysis of an innovative biomass dryer. Renew Energ. 2020;159:860-72.
[14] Norton T, Tiwari B, Sun DW. Computational fluid dynamics in the design and analysis of thermal processes: a review of recent advances. Crit Rev Food Sci Nutr. 2013;53:251-75.

[15] Darabi H, Zomorodian A, Akbari M, Lorestani AN. Design a cabinet dryer with two geometric configurations using CFD. J Food Sci Tech. 2015;52:359-66.
[16] Pintana P, Thanompongchart P, Phimphilai K, Tippayawong N. Improvement of airflow distribution in glutinous rice cracker drying cabinet. Energ Procedia. 2017;138:325-30.
[17] Vivekanandan M, Periasamy K, Babu CD, Selvakumar G, Arivazhagan R. Experimental and CFD investigation of six shapes of solar greenhouse dryer in no load conditions to identify the ideal shape of dryer. Mater Today Proc. 2021;37:1409-16.
[18] Margaris DP, Ghiaus AG. Dried product quality improvement by air flow manipulation in tray dryers. J Food Eng. 2006;75: 542-50.
[19] Brooker DB, Bakker-Arkema FW, Hall CW. Drying and storage of grains and oilseeds. New York: Van Nostrand Reinhold; 1992.
[20] Sundararaj S, Abraham BA, Krishnakumar P. Computational fluid dynamics analysis of flow in diffuser of a desiccant type air dryer. Mater Today Proc. 2021;37:1517-23.
[21] Demissie P, Hayelom M, Kassaye A, Hailesilassie A, Gebrehiwot M, Vanierschot M. Design, development and CFD modeling of indirect solar food dryer. Energ Procedia. 2019;158:1128-34.
[22] Wang V, Jadav A, Munsin R, Yossapong L. Investigation of pre-Injection flow characteristics in constant volume combustion chamber (CVCC) using computational fluid dynamic (CFD). Proceeding of the 5th TSME International Conference on Mechanical Engineering; 2014 Dec 17-19; Chiang Mai, Thailand; 2014.
[23] Anderson JD. Computational fluid dynamics: the basics with applications. New York: McGraw-Hill; 1995.
[24] Zhang Z, Zhang W, Zhai ZJ, Chen QY. Evaluation of various turbulence models in predicting airflow and turbulence in enclosed environments by CFD: part 2-comparison with experimental data from literature. HVAC&R Res. 2007;13(6):871-86.
[25] Mulet A, Berna A, Borr M, Pinaga F. Effect of air flow rate on carrot drying. Drying Tech. 1987;5:245-58.
[26] Karathanos VT, Belessiotis VG. Sun and artificial air drying kinetics of some agricultural products. J Food Eng. 1997;31:35-46.